

RECONSTRUCTION OF HIGH-RESOLUTION VELOCITY FIELDS IN TURBULENT FLOWS FROM LOW-RESOLUTION MEASUREMENTS

LINH VAN NGUYEN

LML FRE 3723, CRISTAL-CNRS UMR 9189
UNIVERSITÉ DE LILLE, 59655 VILLENEUVE D'ASCQ

SEPTEMBER 28, 2016

JURY MEMBERS: DR. ETIENNE MÉMIN
PR. OLIVIER MICHEL
PR. DANAILA LUMINITA
PR. NICOLAS DOBIGEON

SUPERVISORS: DR. JEAN-PHILIPPE LAVAL
DR. PIERRE CHAINAIS



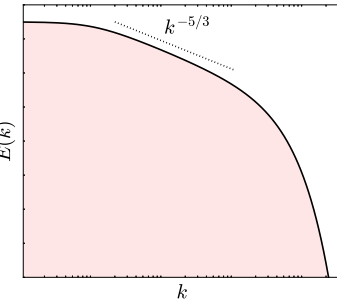
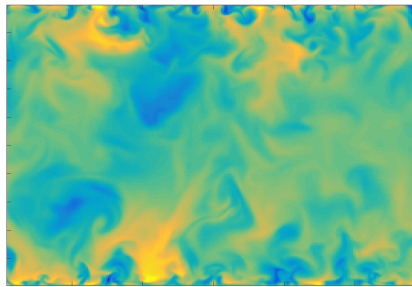
Laboratoire
Mécanique
Lille



- 1 Problem definition
 - Context of the present work
 - Datasets for numerical experiments
 - The two addressed problems
- 2 The proposed approaches
 - Related approaches
 - Mapping functions between large and small scales
 - Fusion of complementary measurements
- 3 Analyses of models performances
 - On isotropic turbulence dataset
 - On turbulent channel flow dataset
- 4 Conclusions and perspectives
 - Conclusions
 - Suggestions for future works
 - Contributions

Turbulence is multiscale

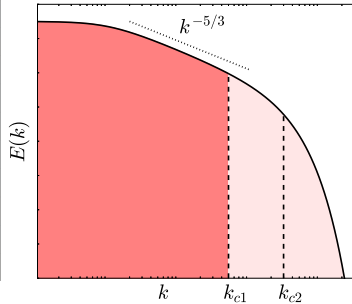
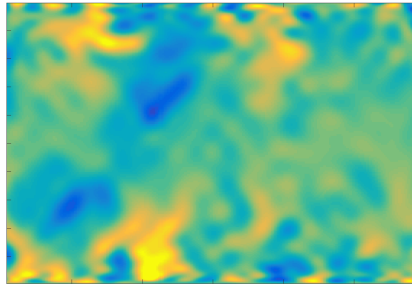
- ▶ **Large scales** carry most of kinetic energy, responsible for flow dynamics and transportation of matter
- ▶ **Small scales** are more related to dissipation properties; more universal



Sample streamwise velocity field of a channel flow ($Re_\tau = 550$) and a synthesized spectrum (all scales)

Turbulence is multiscale

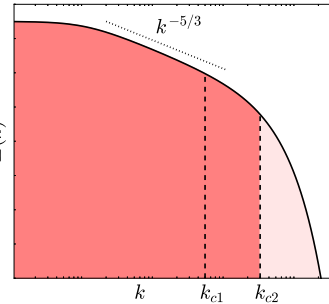
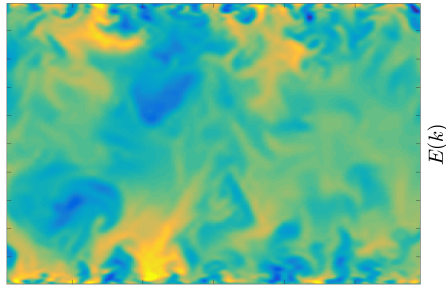
- ▶ **Large scales** carry most of kinetic energy, responsible for flow dynamics and transportation of matter
- ▶ **Small scales** are more related to dissipation properties; more universal



Sample streamwise velocity field of a channel flow ($Re_\tau = 550$) and a synthesized spectrum (large scales)

Turbulence is multiscale

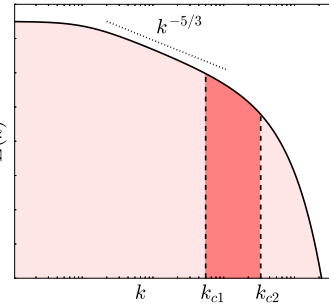
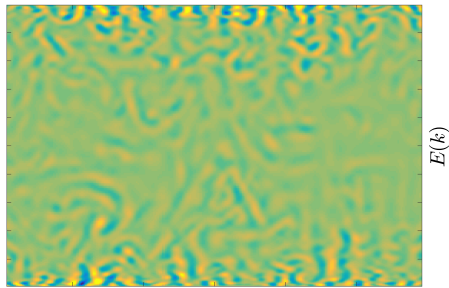
- ▶ **Large scales** carry most of kinetic energy, responsible for flow dynamics and transportation of matter
- ▶ **Small scales** are more related to dissipation properties; more universal



Sample streamwise velocity field of a channel flow ($Re_\tau = 550$) and a synthesized spectrum (large scales)

Turbulence is multiscale

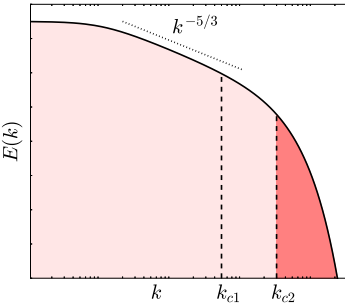
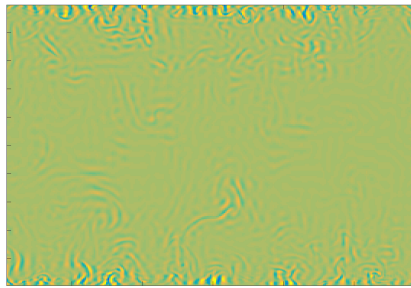
- ▶ **Large scales** carry most of kinetic energy, responsible for flow dynamics and transportation of matter
- ▶ **Small scales** are more related to dissipation properties; more universal



Sample streamwise velocity field of a channel flow ($Re_\tau = 550$) and a synthesized spectrum (mid scales)

Turbulence is multiscale

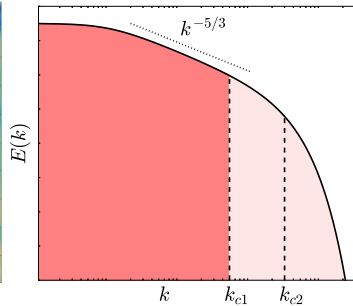
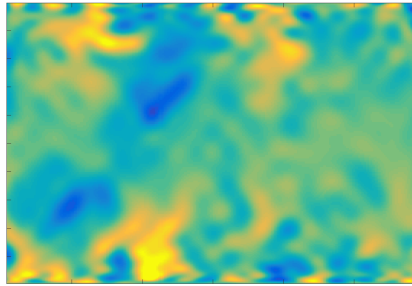
- ▶ **Large scales** carry most of kinetic energy, responsible for flow dynamics and transportation of matter
- ▶ **Small scales** are more related to dissipation properties; more universal



Sample streamwise velocity field of a channel flow ($Re_\tau = 550$) and a synthesized spectrum (small scales)

Turbulence is multiscale

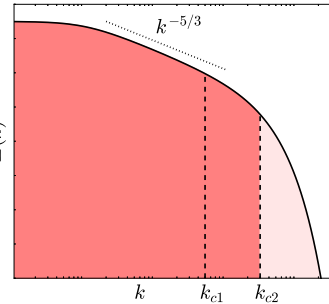
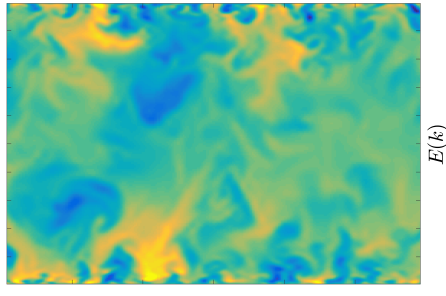
- ▶ **Large scales** carry most of kinetic energy, responsible for flow dynamics and transportation of matter
- ▶ **Small scales** are more related to dissipation properties; more universal



Sample streamwise velocity field of a channel flow ($Re_\tau = 550$) and a synthesized spectrum (large scales)

Turbulence is multiscale

- ▶ **Large scales** carry most of kinetic energy, responsible for flow dynamics and transportation of matter
- ▶ **Small scales** are more related to dissipation properties; more universal



Sample streamwise velocity field of a channel flow ($Re_\tau = 550$) and a synthesized spectrum (large scales)

Importance of small scales

- ▶ Better insight on turbulence physics (dissipation, coherent structures)
- ▶ Validation of turbulence models (Large Eddy Simulation)

Importance of small scales

- ▶ Better insight on turbulence physics (dissipation, coherent structures)
- ▶ Validation of turbulence models (Large Eddy Simulation)



Turbulent boundary layers (photo credit: Juan A. Sillero)

Importance of small scales

- ▶ Better insight on turbulence physics (dissipation, coherent structures)
- ▶ Validation of turbulence models (Large Eddy Simulation)



Turbulent combustion and reacting flows (photo credit: TESLa, Colorado University)

Motivations of the thesis

Problem: cannot access a full range of scales

- ▶ **Experiments:**
 - ▶ **Optical measurement** (PIV, PTV): compromise between frequency, resolution and field-of-view
 - ▶ **Hot wire anemometer** (HWA): high frequency but point-measurement
- ▶ **Simulations:** only accessible from Direct Numerical Simulation, but
 - ▶ limited to low to moderate Re and/or simple geometries
 - ▶ excessive computational cost to converge statistics

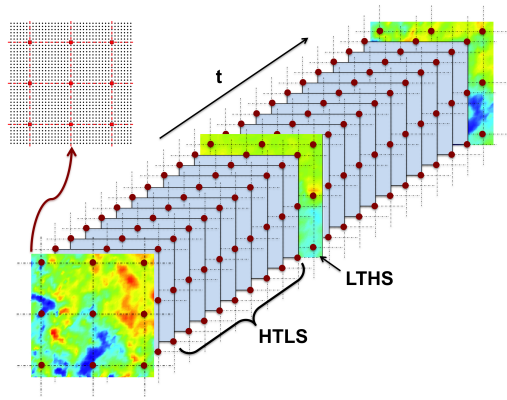
Our main objectives:

- ▶ Computational methods to reconstruct partly unresolved scales
- ▶ Model assessment using numerical database

Numerical experiment setup

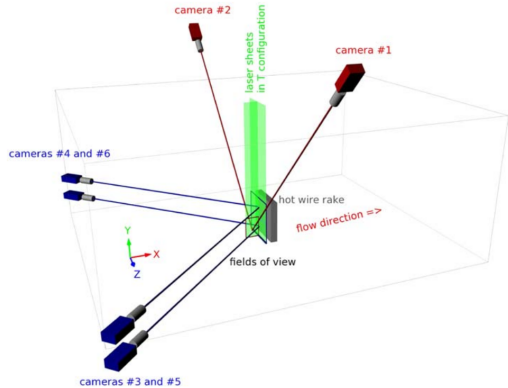
Setup of complementary measurements:

- ▶ High-Time-Low-Space (**HTLS**) of size $Q \times N$
- ▶ Low-Time-High-Space (**LTHS**) of size $P \times M$ ($Q \ll P, M \ll N$)



Example: WALLTURB project [Coudert et al., 2011]

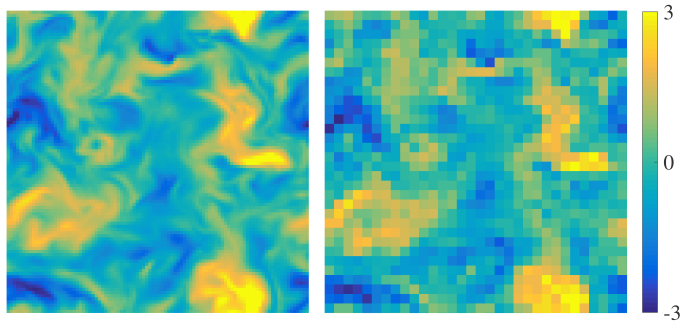
- ▶ Complementary measurements: **HWA** as **HTLS** (11×13 , 30 kHz), **PIV** as **LTHS** (143×161 , 4 Hz)
- ▶ Reconstruct **HTHS** (143×161 , 30 kHz) using regression
[Dekou et al., 2016]



Numerical datasets

Two numerical datasets of full resolution are used:

- (i.) **Isotropic turbulence**: 37 blocks of 3D field of 96^3 ($Re_\lambda = 90, 384^3$)
- (ii.) **Turbulent channel flow**: 10000 snapshots of 257×288 , $Re_\tau = 550$

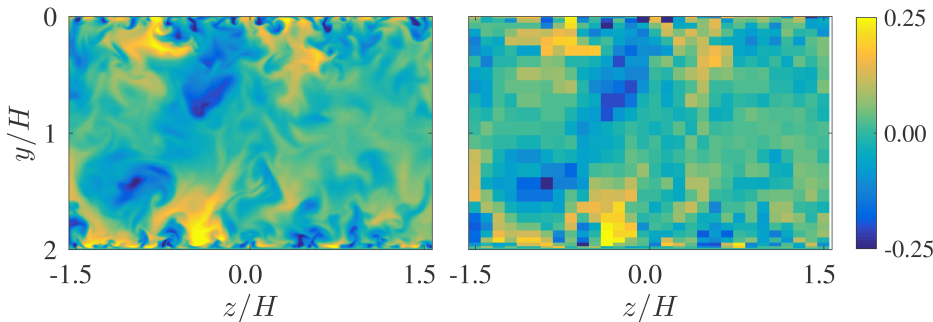


Sample streamwise velocity field of isotropic turbulence at $Re_\lambda = 90$

Numerical datasets

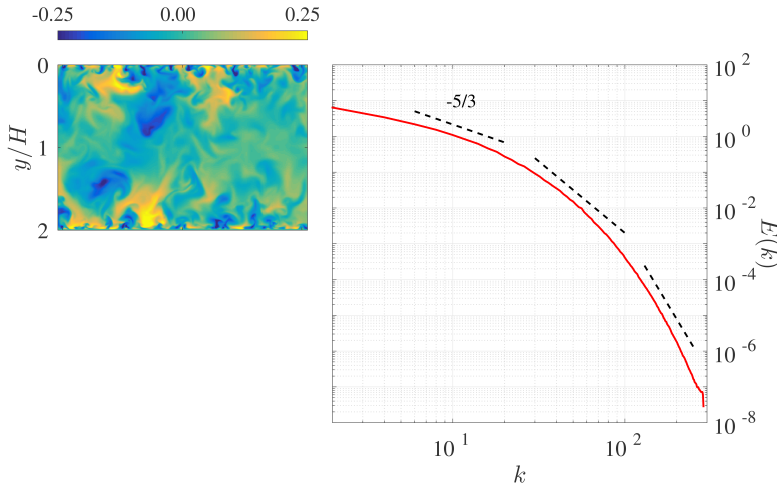
Two numerical datasets of full resolution are used:

- (i.) **Isotropic turbulence**: 37 blocks of 3D field of 96^3 ($Re_\lambda = 90, 384^3$)
- (ii.) **Turbulent channel flow**: 10000 snapshots of 257×288 , $Re_\tau = 550$



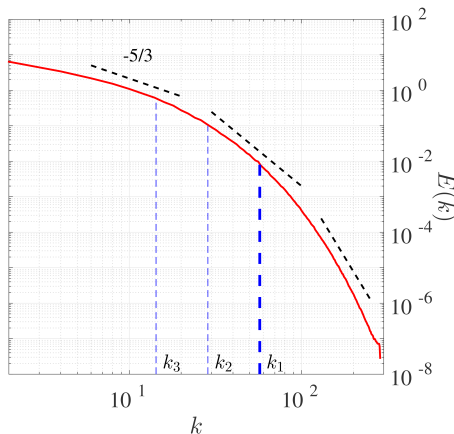
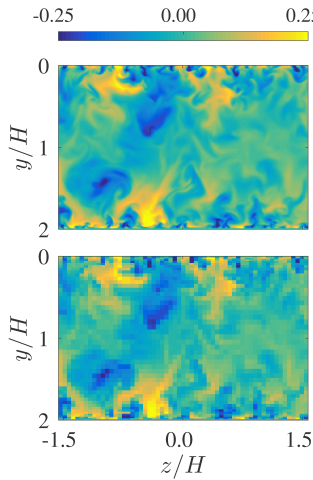
Sample streamwise velocity field of the channel flow at $Re_\tau = 550$

Problem definition: inverse problem



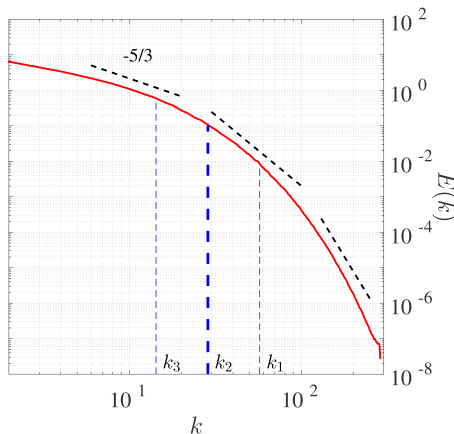
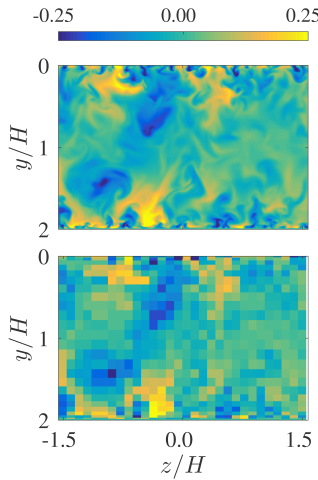
A sample streamwise velocity field from DNS of a turbulent channel flow ($Re_\tau = 550$) and the spectrum in space

Problem definition: inverse problem



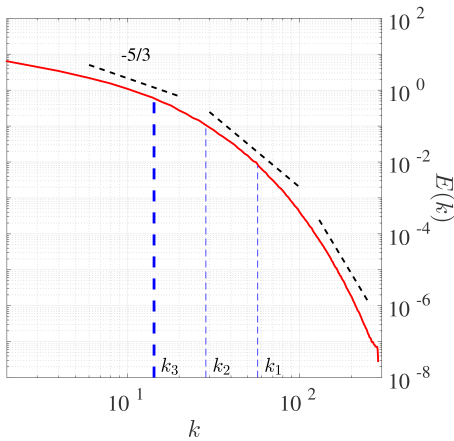
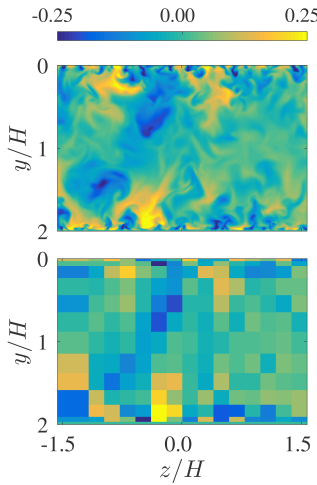
Subsample by 5×5 (k_1)

Problem definition: inverse problem



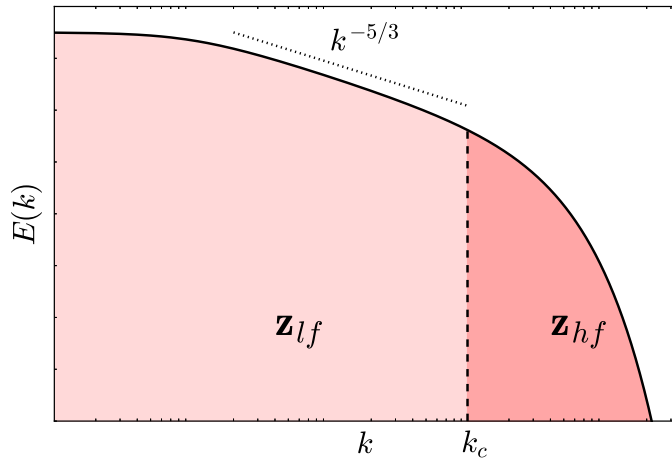
Subsample by 10×10 (k_2)

Problem definition: inverse problem

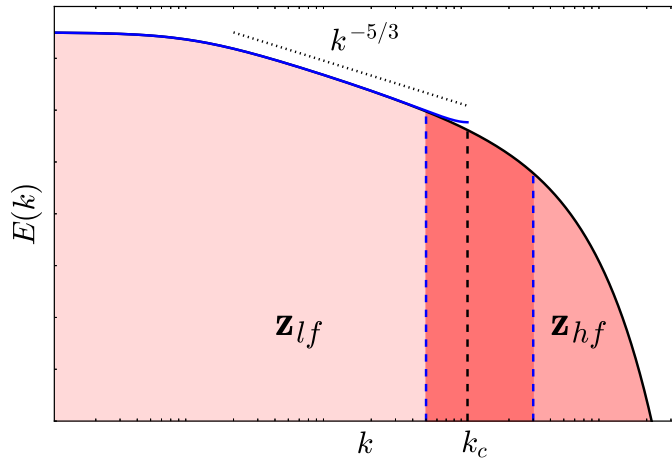


Subsample by $20 \times 20 (k_3)$

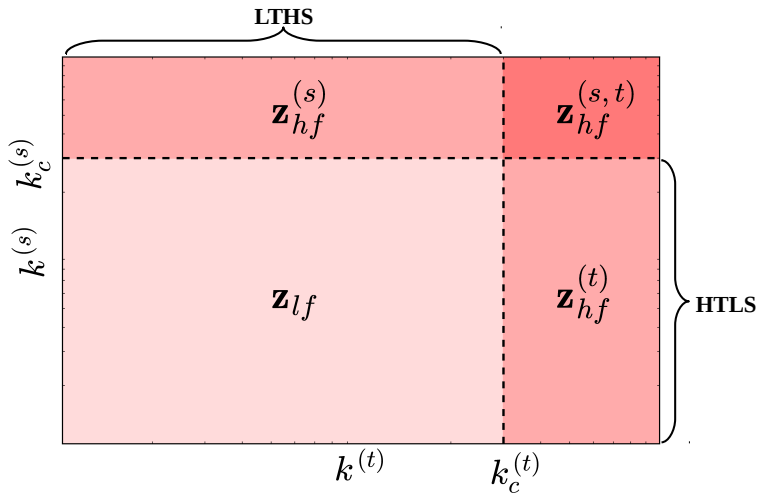
Problem 1: mapping functions between small & large scales



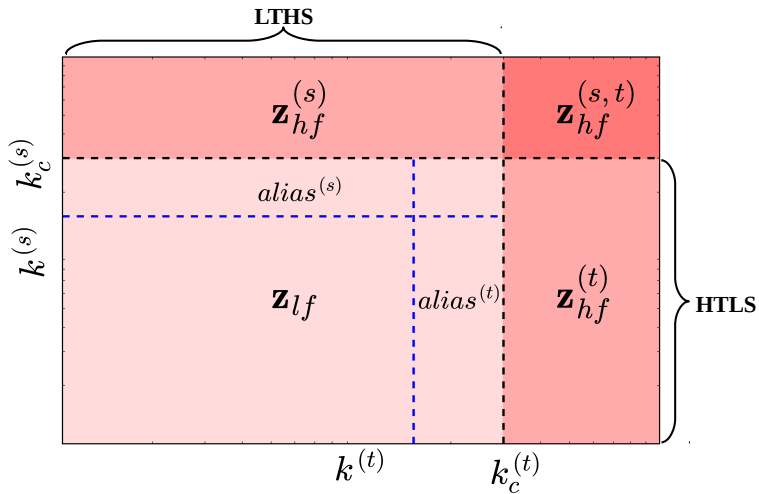
Problem 1: mapping functions between small & large scales



Problem 2: fusion of complementary measurements



Problem 2: fusion of complementary measurements



Related approaches in the literature

Reconstruction methods in turbulence studies:

- ▶ **Least-square** regression [Durgesh and Naughton, 2010]
- ▶ **POD** reduced-order model [Bonnet et al., 1994]
- ▶ **Data assimilation** using Kalman filter [Papadakis et al., 2010, Tu et al., 2013]
- ▶ **Physical priors**: div-curl regularization [Corpetti et al., 2002],
vortex-in-cell [Schneiders et al., 2014]

Related approaches in the literature

Reconstruction methods in turbulence studies:

- **Least-square** regression [Durgesh and Naughton, 2010]
- **POD** reduced-order model [Bonnet et al., 1994]
- **Data assimilation** using Kalman filter [Papadakis et al., 2010, Tu et al., 2013]
- **Physical priors**: div-curl regularization [Corpetti et al., 2002],
vortex-in-cell [Schneiders et al., 2014]



Approaches in the present work

Approach 1: learn a mapping function between scales

Objective: $\mathbf{z}_\ell \in \mathbb{R}^Q \mapsto \mathbf{z}_h \in \mathbb{R}^P, P \gg Q$

- ▶ **Regression:** as set of coefficients
- ▶ **Coupled dictionary learning:** coupled representations of LR/HR

Approach 2: fusion of complementary measurements

Objective: find \mathbf{z} given two measurements \mathbf{x} and \mathbf{y}

- ▶ **Non-local means:** self similarity of flow structures
- ▶ **Bayesian fusion:** *maximum a posteriori* estimate $p(\mathbf{z} | \mathbf{x}, \mathbf{y})$

Regression

Learn f from training samples $(\mathbf{y}_t, \mathbf{z}_t)$:

$$f : \mathbf{y}_t \mapsto \hat{\mathbf{z}}_t = f(\mathbf{y}_t) + \mathbf{n}^{(t)} \approx \mathbf{B}^\top \mathbf{y}_t$$

- ▶ Linear regression:

$$\mathbf{B} = \underset{\mathbf{B}}{\operatorname{argmin}} \left\{ \underbrace{\|\mathbf{Y}\mathbf{B} - \mathbf{Z}\|_2^2}_{\text{data misfit}} + \underbrace{\lambda g(\mathbf{B})}_{\text{penalty}} \right\}$$

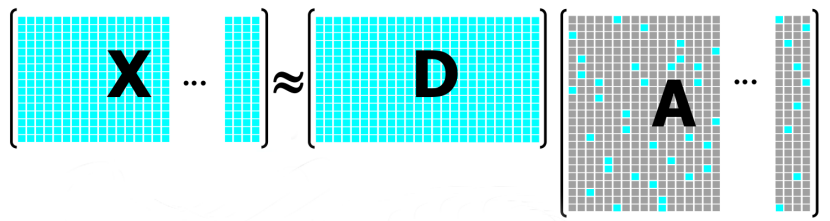
- ▶ **Ridge regression**: $g(\mathbf{B}) = \|\mathbf{B}\|_2^2$
- ▶ **LASSO**: $g(\mathbf{B}) = \|\mathbf{B}\|_1$
- ▶ Nonlinear regression: projection into kernel space (**KRR**)
- ▶ Parameter estimation: *bias-variance* trade-off, *k-fold* cross validation

Dictionary learning: a generalization of POD

- ▶ Data representation: linear transformation via a “*dictionary*”

$$\mathbf{X} = \mathbf{D}\mathbf{A}$$

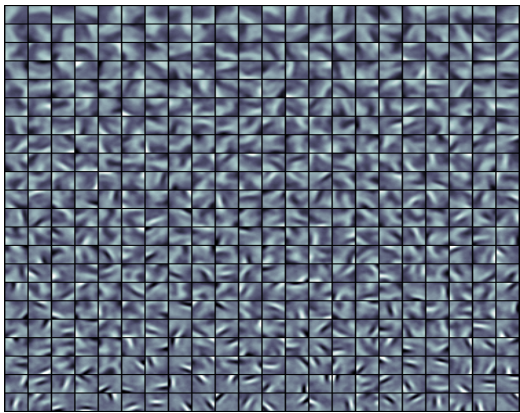
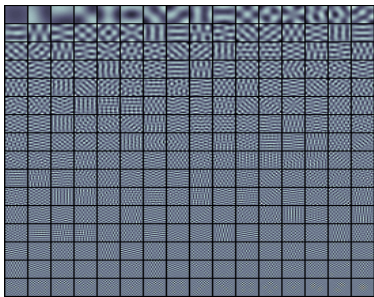
- ▶ Dictionary learning: \mathbf{D} is *redundant* (or *overcomplete*), \mathbf{A} is *sparse*



- ▶ Dictionary learning as an alternating optimization problem:

$$(\mathbf{D}, \mathbf{A}) = \operatorname{argmin}_{\mathbf{D}, \mathbf{A}} \left\{ \|\mathbf{X} - \mathbf{D}\mathbf{A}\|_2^2 + \lambda \|\mathbf{A}\|_1 \right\}$$

Orthogonal vs redundant bases

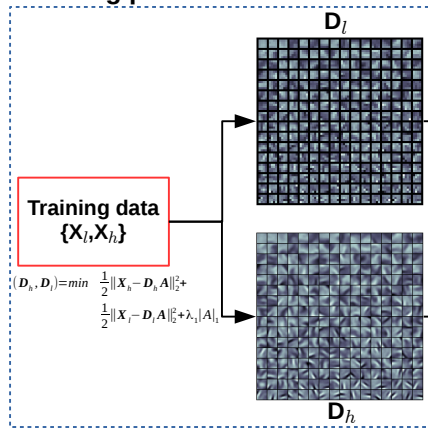


Dictionaries learned by POD and DL from the set of HR patches of size 16×16

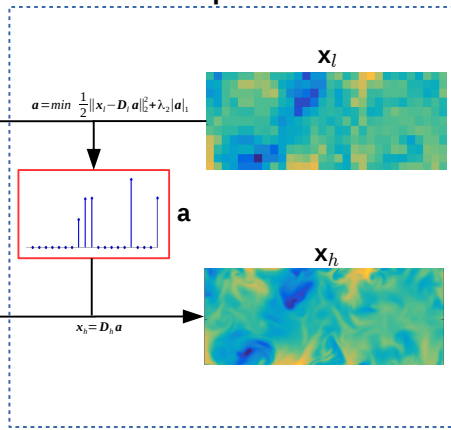
Reconstruct HR fields using coupled dictionary learning

- Motivated by single image super-resolution [Yang et al., 2010]
- Two steps: *learning* (offline) and *reconstruction* (online)

Learning phase



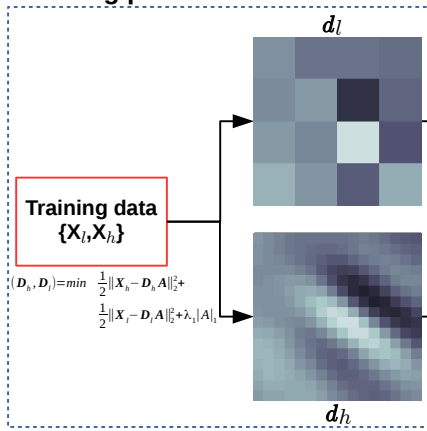
Reconstruction phase



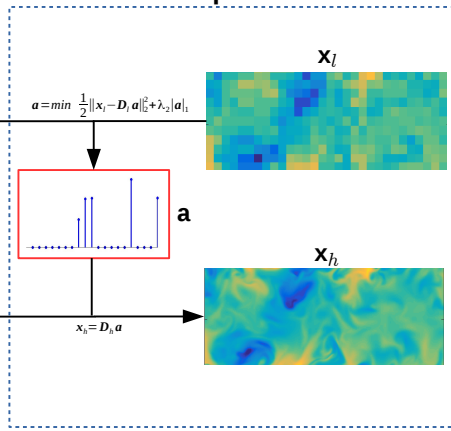
Reconstruct HR fields using coupled dictionary learning

- Motivated by single image super-resolution [Yang et al., 2010]
- Two steps: *learning* (offline) and *reconstruction* (online)

Learning phase



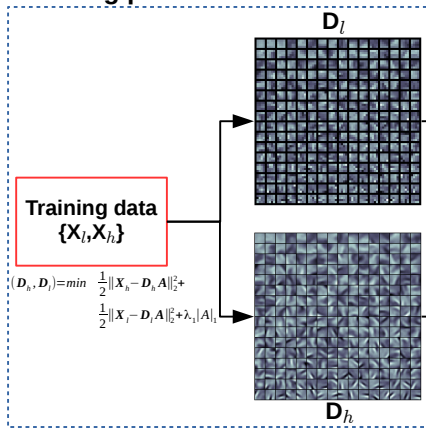
Reconstruction phase



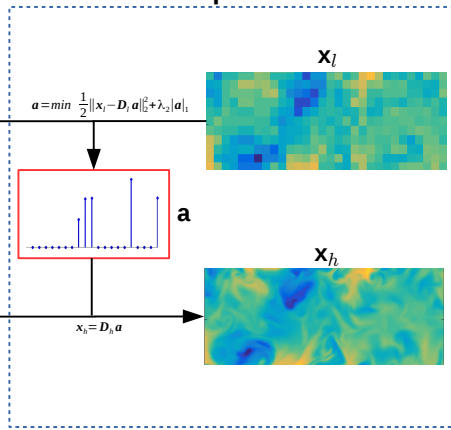
Reconstruct HR fields using coupled dictionary learning

- Motivated by single image super-resolution [Yang et al., 2010]
- Two steps: *learning* (offline) and *reconstruction* (online)

Learning phase



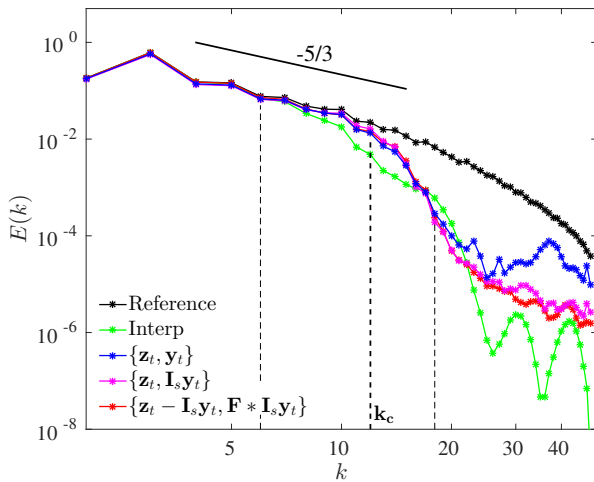
Reconstruction phase



Numerical experiment setup for coupled dictionary learning

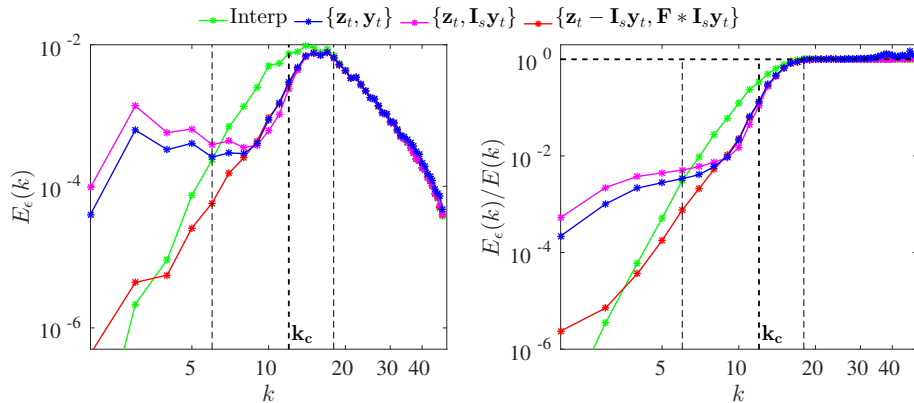
- ▶ **Subsampling:** $y_t \triangleq \mathbb{S}_s z_t$
- ▶ **Downsampling case:** $y_t \triangleq \mathbb{S}_s \mathbb{L}_s z_t$
- ▶ **Patch-based approach:** localized information
- ▶ **Parameters:** patch size, number of patches, sparsity constraints (for the learning and reconstruction step)
- ▶ **Preprocessing methods** by coupling:
 - ▶ High and low resolution, $\{z_t, y_t\}$
 - ▶ Reference and interpolated high resolution, $\{z_t, \mathbb{I}_s y_t\}$
 - ▶ Residual and features (derivatives), $\{z_t - \mathbb{I}_s y_t, \mathbb{F} * \mathbb{I}_s y_t\}$

Results: energy spectra



Energy spectra (2D) of reference, interpolation and reconstruction by 3 coupled dictionary learning approaches (sampling ratio of 4×4)

Results: spectra of the error



2D error spectra (with and without normalization) of interpolation and reconstruction by 3 coupled dictionary learning approaches (sampling ratio of 4×4)

Approaches in the present work

Approach 1: learn a mapping function between scales

Objective: $z_\ell \in \mathbb{R}^Q \mapsto z_h \in \mathbb{R}^P, P \gg Q$

- ▶ **Regression:** as set of coefficients
- ▶ **Coupled dictionary learning:** coupled representations of LR/HR

Approach 2: fusion of complementary measurements

Objective: find z given two measurements x and y

- ▶ **Non-local means:** self similarity of flow structures
- ▶ **Bayesian fusion:** *maximum a posteriori* estimate $p(z|x, y)$

A generalization of non-local means

Objective: propagating small scales from LTHS planes based on the similarity levels between large scales

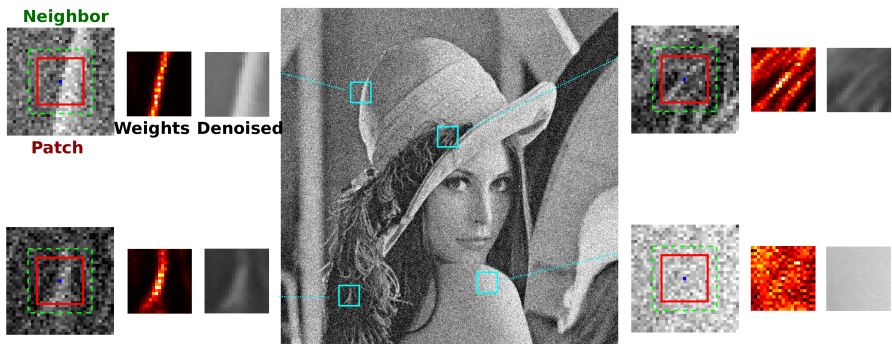


Figure: Non-local means for denoising [Buades et al., 2005]

A generalization of non-local means

Objective: propagating small scales from LTHS planes based on the similarity levels between large scales

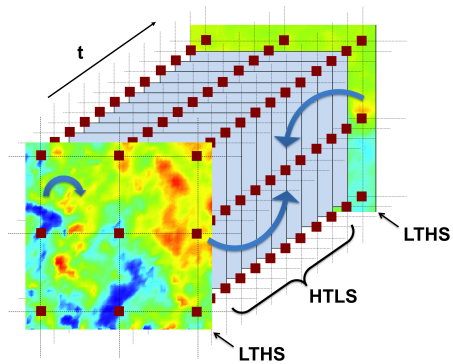


Figure: Propagation of small scales, inspired by video super-resolution [Protter et al., 2009]

The principle: weighted average using non-local similarity

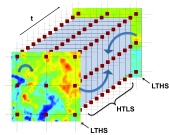
- ▶ **Principle:** video super-resolution [Protter et al., 2009]

$$\hat{\mathbf{z}}_{t_o}[k] = \frac{\sum_{t \in \mathcal{N}_{t_o}} \sum_{i \in \mathcal{N}_k} w[k, i, t] \mathbf{y}_t[i]}{\sum_{t \in \mathcal{N}_{t_o}} \sum_{i \in \mathcal{N}_k} w[k, i, t]}$$

where $w[k, i, t] = \exp\left(-\frac{1}{2\sigma^2} \|\mathcal{R}_s^k \mathbf{y}_{t_o} - \mathcal{R}_s^i \mathbf{y}_t\|_2^2\right)$

- ▶ **Modification:** reconstruct small scales $\mathbf{b}_{t_o} = \mathbf{x}_{t_o} - \mathbb{I}_s \mathbb{S}_s \mathbf{x}_{t_o}$ only

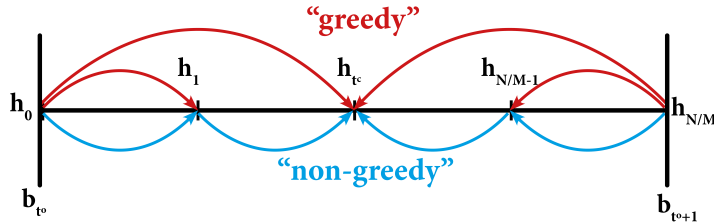
$$\hat{\mathbf{b}}_t[k] = \frac{\sum_{i \in \mathcal{N}_k} w_0[k, i, t] \mathbf{b}_{t_o}[i] + \sum_{i \in \mathcal{N}_k} w_1[k, i, t] \mathbf{b}_{t_o+1}[i]}{\sum_{i \in \mathcal{N}_k} w_0[k, i, t] + \sum_{i \in \mathcal{N}_k} w_1[k, i, t]}$$



Non-local means: schemes and parameters

► Parameters:

- ▶ Filter parameter: σ
- ▶ Neighbor size #(N_k)
- ▶ Patch size: #($\mathcal{R}_s^k y_t$)
- ▶ Greedy and non-greedy propagation schemes



Bayesian fusion: the framework

- ▶ Motivation: fusion of multi- and hyper-spectral images [Hardie et al., 2004]
- ▶ Bayesian fusion: *maximum a posteriori*

$$\hat{\mathbf{z}} = \operatorname{argmax}_{\mathbf{z}} \{ p(\mathbf{z} | \mathbf{x}, \mathbf{y}) \}$$

- ▶ Applying *Bayes' theorem*:

$$p(\mathbf{z} | \mathbf{x}, \mathbf{y}) = \frac{p(\mathbf{x}, \mathbf{y} | \mathbf{z}) p(\mathbf{z})}{p(\mathbf{x}, \mathbf{y})} = \frac{p(\mathbf{x} | \mathbf{z}) p(\mathbf{y} | \mathbf{z}) p(\mathbf{z})}{p(\mathbf{x}, \mathbf{y})}$$

- ▶ *Non-informative (improper) prior*, i.e. $p(\mathbf{z})$ is constant,:

$$\hat{\mathbf{z}} = \operatorname{argmax}_{\mathbf{z}} \{ p(\mathbf{z} | \mathbf{x}) p(\mathbf{z} | \mathbf{y}) \}$$

Single models and closed-form fusion formula

- ▶ Single models:

$$\mathbf{z} = \mathbb{I}_t \mathbf{x} + \mathbf{h}_t \quad (\mathbb{I}_t \mathbf{x} \perp\!\!\!\perp \mathbf{h}_t)$$

$$\mathbf{z} = \mathbb{I}_s \mathbf{y} + \mathbf{h}_s \quad (\mathbb{I}_s \mathbf{y} \perp\!\!\!\perp \mathbf{h}_s)$$

- ▶ Multivariate Gaussian probability:

$$p(\mathbf{z} | \mathbf{x}) = \frac{1}{(2\pi)^{PN/2} |\Sigma_{\mathbf{h}_t}|^{1/2}} \exp \left\{ -\frac{1}{2} (\mathbf{z} - \mathbb{I}_t \mathbf{x})^\top \Sigma_{\mathbf{h}_t}^{-1} (\mathbf{z} - \mathbb{I}_t \mathbf{x}) \right\}$$

($\Sigma_{\mathbf{h}_t} = \mathbf{h}_t \mathbf{h}_t^\top$: covariance matrix)

- ▶ Closed-form solution:

$$\hat{\mathbf{z}} = \left(\Sigma_{\mathbf{h}_s}^{-1} + \Sigma_{\mathbf{h}_t}^{-1} \right)^{-1} \left(\Sigma_{\mathbf{h}_s}^{-1} \mathbb{I}_s \mathbf{y} + \Sigma_{\mathbf{h}_t}^{-1} \mathbb{I}_t \mathbf{x} \right)$$

Simplification and interpretation of the fusion formula

Simplification: Σ_{h_s} and Σ_{h_t} are diagonal

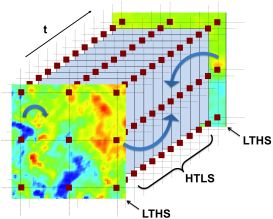
$$\hat{\mathbf{z}}[i, t] = \frac{\sigma_{h_s}^2[i, t]}{\sigma_{h_s}^2[i, t] + \sigma_{h_t}^2[i, t]} \mathbb{I}_t \mathbf{x}[i, t] + \frac{\sigma_{h_t}^2[i, t]}{\sigma_{h_s}^2[i, t] + \sigma_{h_t}^2[i, t]} \mathbb{I}_s \mathbf{y}[i, t]$$

Simplification and interpretation of the fusion formula

Simplification: Σ_{h_s} and Σ_{h_t} are diagonal

$$\hat{\mathbf{z}}[i, t] = \frac{\sigma_{h_s}^2[i, t]}{\sigma_{h_s}^2[i, t] + \sigma_{h_t}^2[i, t]} \mathbb{I}_t \mathbf{x}[i, t] + \frac{\sigma_{h_t}^2[i, t]}{\sigma_{h_s}^2[i, t] + \sigma_{h_t}^2[i, t]} \mathbb{I}_s \mathbf{y}[i, t]$$

Interpretation: $\hat{\mathbf{z}}$ is fused from 2 data sources $\mathbb{I}_t \mathbf{x}$ and $\mathbb{I}_s \mathbf{y}$ via weighted coefficients $\sigma_{h_s}^2$ and $\sigma_{h_t}^2$ (learned from \mathbf{x} and \mathbf{y} only).

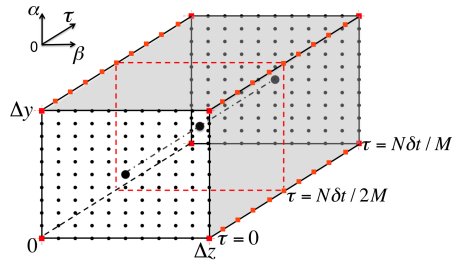


Models performances: loss of energy and NRMSE

$\hat{\mathbf{z}}$, $\tilde{\mathbf{z}}$ and $\mathbb{L} \mathbf{z}$ are reference, reconstructed and filtered fields

- ▶ Loss of energy:

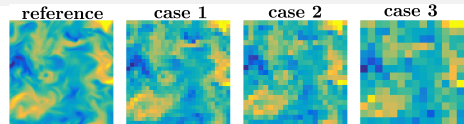
$$\Delta\kappa = \frac{\sum_{j \in \mathbb{J}} \mathbf{z}_j^2 - \sum_{j \in \mathbb{J}} [\mathbb{L} \mathbf{z}]_j^2}{\sum_{j \in \mathbb{J}} \mathbf{z}_j^2}$$



- ▶ Normalized Root Mean Squared Error (NRMSE):

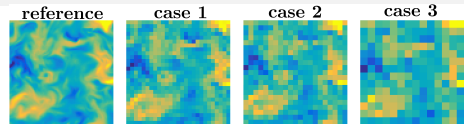
$$\epsilon = \left(\frac{\sum_t \sum_{j \in \mathbb{J}} (\hat{\mathbf{z}}_{t,j} - \mathbf{z}_{t,j})^2}{\sum_t \sum_{j \in \mathbb{J}} \mathbf{z}_{t,j}^2} \right)^{1/2}$$

NRMSEs on isotropic turbulence data



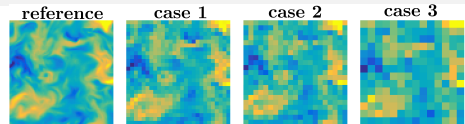
| Method | $(\frac{P}{Q}, \frac{N}{M})$ $\Delta\kappa$ | $\bar{\epsilon}$ | | | ϵ_{max} | | |
|---------------------------|--|------------------|------------------|------------------|------------------|------------------|------------------|
| | | Case 1 | Case 2 | Case 3 | Case 1 | Case 2 | Case 3 |
| | | $(3^2, 4)$ 1% | $(4^2, 6)$ 3% | $(6^2, 8)$ 7% | $(3^2, 4)$ 1% | $(4^2, 6)$ 3% | $(6^2, 8)$ 7% |
| $\mathbb{I}_s \mathbf{y}$ | | 0.19 | 0.28 | 0.43 | 0.22 | 0.35 | 0.52 |
| $\mathbb{I}_t \mathbf{x}$ | | 0.13 | 0.23 | 0.31 | 0.19 | 0.28 | 0.42 |
| RR | | 0.14 | 0.23 | 0.35 | 0.20 | 0.34 | 0.50 |
| KRR | | 0.13 | 0.23 | 0.34 | 0.20 | 0.34 | 0.49 |
| Greedy propag | | 0.11 | 0.20 | 0.32 | 0.18 | 0.33 | 0.51 |
| Non-greedy propag | | 0.11 | 0.19 | 0.30 | 0.17 | 0.31 | 0.46 |
| Fusion (LG) | | 0.11 | 0.18 | 0.27 | 0.17 | 0.26 | 0.41 |
| Fusion (BF) | | 0.11 | 0.18 | 0.26 | 0.17 | 0.26 | 0.40 |

NRMSEs on isotropic turbulence data



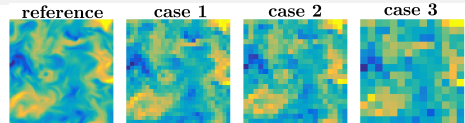
| Method | $(\frac{P}{Q}, \frac{N}{M})$ $\Delta\kappa$ | $\bar{\epsilon}$ | | | ϵ_{max} | | |
|---------------------------|--|------------------|------------------|------------------|------------------|------------------|------------------|
| | | Case 1 | Case 2 | Case 3 | Case 1 | Case 2 | Case 3 |
| | | $(3^2, 4)$ 1% | $(4^2, 6)$ 3% | $(6^2, 8)$ 7% | $(3^2, 4)$ 1% | $(4^2, 6)$ 3% | $(6^2, 8)$ 7% |
| $\mathbb{I}_s \mathbf{y}$ | | 0.19 | 0.28 | 0.43 | 0.22 | 0.35 | 0.52 |
| $\mathbb{I}_t \mathbf{x}$ | | 0.13 | 0.23 | 0.31 | 0.19 | 0.28 | 0.42 |
| RR | | 0.14 | 0.23 | 0.35 | 0.20 | 0.34 | 0.50 |
| KRR | | 0.13 | 0.23 | 0.34 | 0.20 | 0.34 | 0.49 |
| Greedy propag | | 0.11 | 0.20 | 0.32 | 0.18 | 0.33 | 0.51 |
| Non-greedy propag | | 0.11 | 0.19 | 0.30 | 0.17 | 0.31 | 0.46 |
| Fusion (LG) | | 0.11 | 0.18 | 0.27 | 0.17 | 0.26 | 0.41 |
| Fusion (BF) | | 0.11 | 0.18 | 0.26 | 0.17 | 0.26 | 0.40 |

NRMSEs on isotropic turbulence data



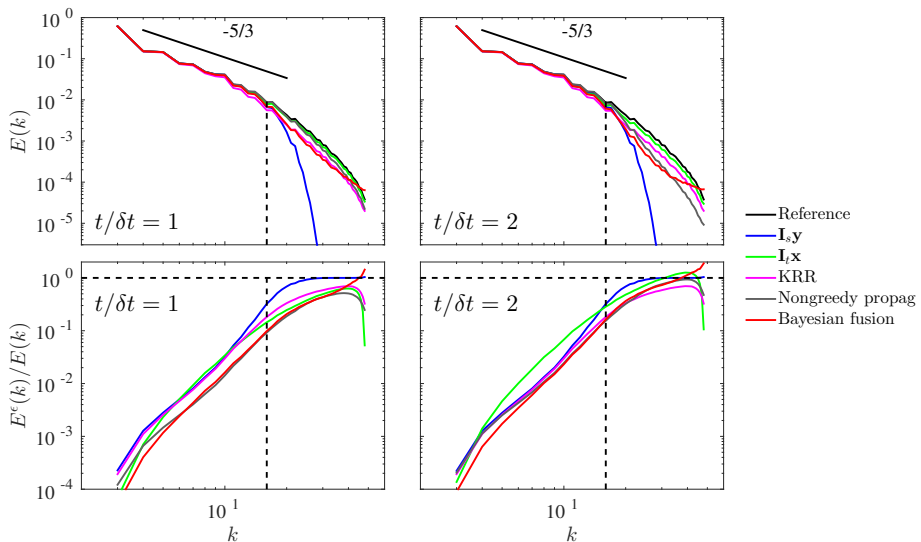
| Method | $(\frac{P}{Q}, \frac{N}{M})$ $\Delta\kappa$ | $\bar{\epsilon}$ | | | ϵ_{max} | | |
|---------------------------|--|------------------|------------------|------------------|------------------|------------------|------------------|
| | | Case 1 | Case 2 | Case 3 | Case 1 | Case 2 | Case 3 |
| | | $(3^2, 4)$ 1% | $(4^2, 6)$ 3% | $(6^2, 8)$ 7% | $(3^2, 4)$ 1% | $(4^2, 6)$ 3% | $(6^2, 8)$ 7% |
| $\mathbb{I}_s \mathbf{y}$ | | 0.19 | 0.28 | 0.43 | 0.22 | 0.35 | 0.52 |
| $\mathbb{I}_t \mathbf{x}$ | | 0.13 | 0.23 | 0.31 | 0.19 | 0.28 | 0.42 |
| RR | | 0.14 | 0.23 | 0.35 | 0.20 | 0.34 | 0.50 |
| KRR | | 0.13 | 0.23 | 0.34 | 0.20 | 0.34 | 0.49 |
| Greedy propag | | 0.11 | 0.20 | 0.32 | 0.18 | 0.33 | 0.51 |
| Non-greedy propag | | 0.11 | 0.19 | 0.30 | 0.17 | 0.31 | 0.46 |
| Fusion (LG) | | 0.11 | 0.18 | 0.27 | 0.17 | 0.26 | 0.41 |
| Fusion (BF) | | 0.11 | 0.18 | 0.26 | 0.17 | 0.26 | 0.40 |

NRMSEs on isotropic turbulence data



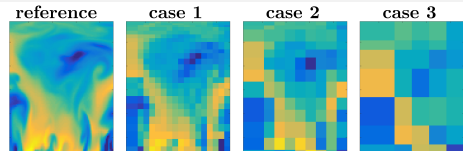
| Method | $(\frac{P}{Q}, \frac{N}{M})$ $\Delta\kappa$ | $\bar{\epsilon}$ | | | ϵ_{max} | | |
|---------------------------|--|------------------|------------------|------------------|------------------|------------------|------------------|
| | | Case 1 | Case 2 | Case 3 | Case 1 | Case 2 | Case 3 |
| | | $(3^2, 4)$ 1% | $(4^2, 6)$ 3% | $(6^2, 8)$ 7% | $(3^2, 4)$ 1% | $(4^2, 6)$ 3% | $(6^2, 8)$ 7% |
| $\mathbb{I}_s \mathbf{y}$ | | 0.19 | 0.28 | 0.43 | 0.22 | 0.35 | 0.52 |
| $\mathbb{I}_t \mathbf{x}$ | | 0.13 | 0.23 | 0.31 | 0.19 | 0.28 | 0.42 |
| RR | | 0.14 | 0.23 | 0.35 | 0.20 | 0.34 | 0.50 |
| KRR | | 0.13 | 0.23 | 0.34 | 0.20 | 0.34 | 0.49 |
| Greedy propag | | 0.11 | 0.20 | 0.32 | 0.18 | 0.33 | 0.51 |
| Non-greedy propag | | 0.11 | 0.19 | 0.30 | 0.17 | 0.31 | 0.46 |
| Fusion (LG) | | 0.11 | 0.18 | 0.27 | 0.17 | 0.26 | 0.41 |
| Fusion (BF) | | 0.11 | 0.18 | 0.26 | 0.17 | 0.26 | 0.40 |

Spectra of reconstructed fields by various methods



Spectral analyses (in space) for case 1, $(P/Q, N/M) = (3^2, 4)$, for planes close to LTHS ($t/\delta t = 1$) or central planes ($t/\delta t = 2$)

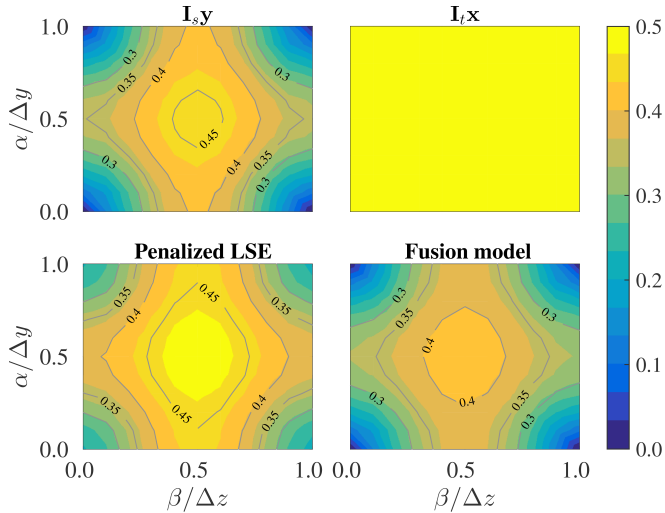
NRMSEs on turbulent channel flow data



| Method | $\bar{\epsilon}$ | | | ϵ_{max} | | |
|---------------------------|------------------------------|-------------|--------------|------------------|-------------|--------------|
| | Case 1 | Case 2 | Case 3 | Case 1 | Case 2 | Case 3 |
| | $(\frac{P}{Q}, \frac{N}{M})$ | $(5^2, 4)$ | $(10^2, 10)$ | $(20^2, 20)$ | $(5^2, 4)$ | $(10^2, 10)$ |
| $\mathbb{I}_s \mathbf{y}$ | 0.14 | 0.36 | 0.68 | 0.16 | 0.47 | 0.85 |
| $\mathbb{I}_t \mathbf{x}$ | 0.11 | 0.32 | 0.54 | 0.18 | 0.55 | 0.85 |
| RR | 0.12 | 0.34 | 0.64 | 0.15 | 0.49 | 0.78 |
| Fusion (BF) | 0.08 | 0.25 | 0.46 | 0.13 | 0.43 | 0.73 |

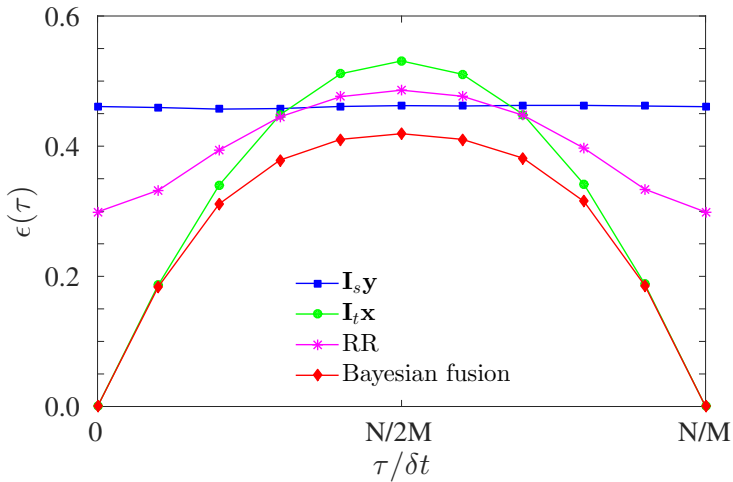
*Errors are estimated in the middle of the channel, $y/H = [0.5, 1.5]$

NRMSEs as functions of position in space



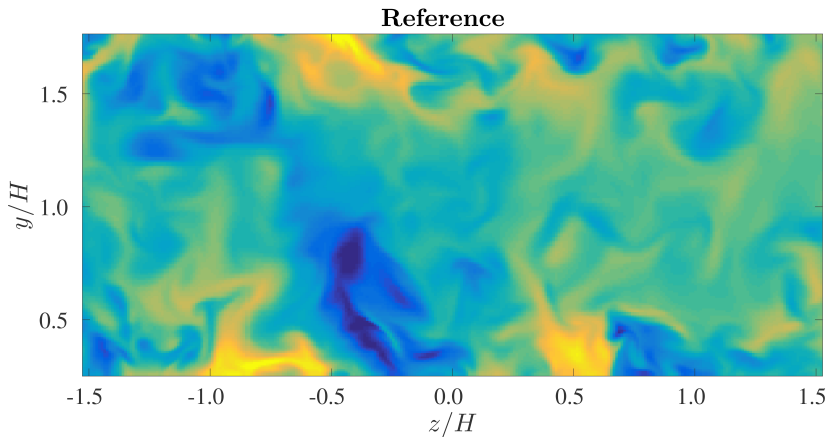
Case 2, $(P/Q, N/M) = (10^2, 10)$: NRMSEs averaged over all points at $y/H = [0.5, 1.5]$ and $(\alpha, \beta) = (\Delta\alpha/2, \Delta\beta/2)$

NRMSEs as functions of position in time

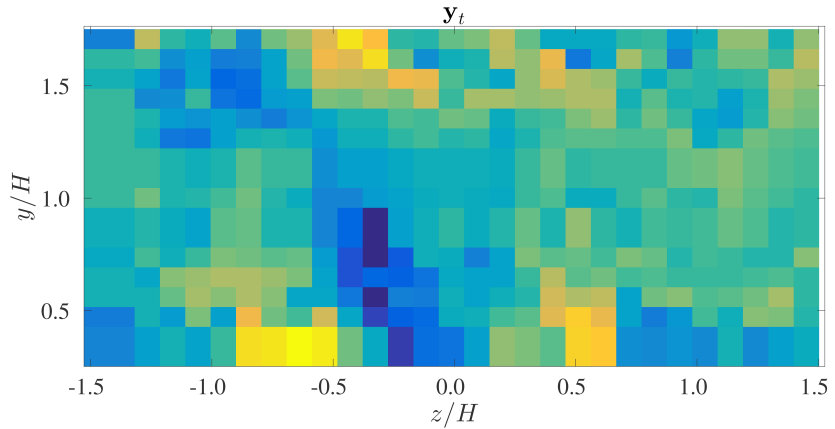


Case 2, $(P/Q, N/M) = (10^2, 10)$: NRMSEs averaged over all blocks bounded by 4 HTLS measurements at $y/H = [0.5, 1.5]$ and $\tau = N/2M$

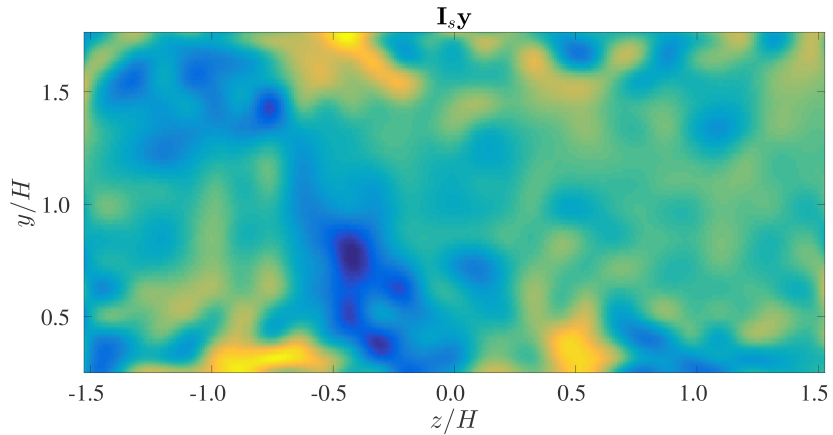
A sample velocity field, $\tau/\delta t = 2$



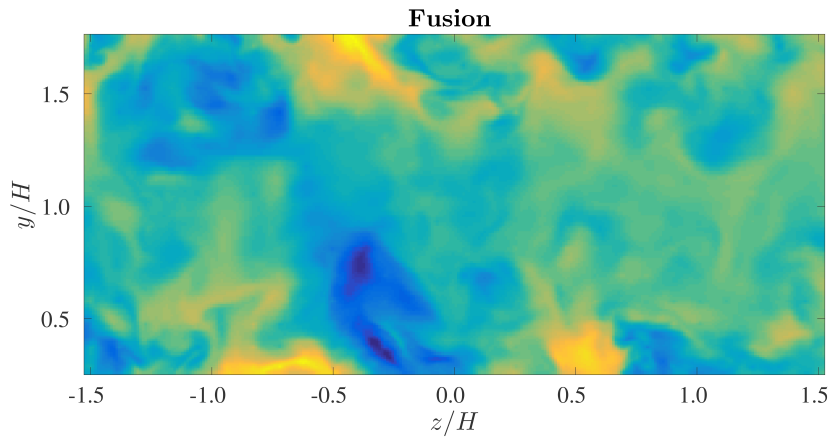
A sample velocity field, $\tau/\delta t = 2$



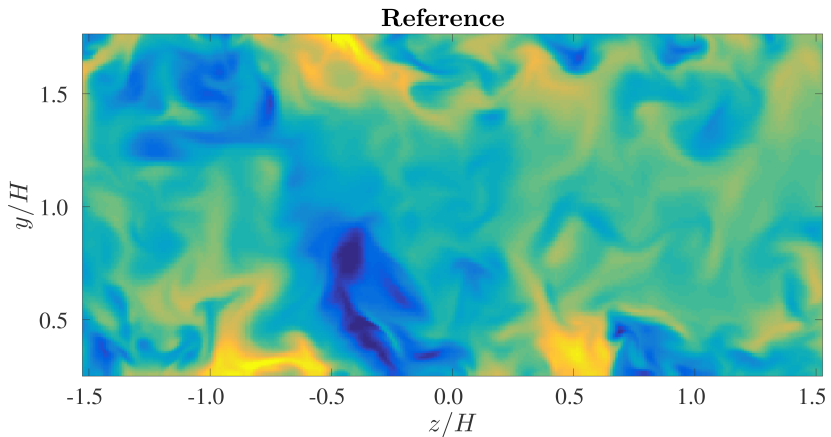
A sample velocity field, $\tau/\delta t = 2$



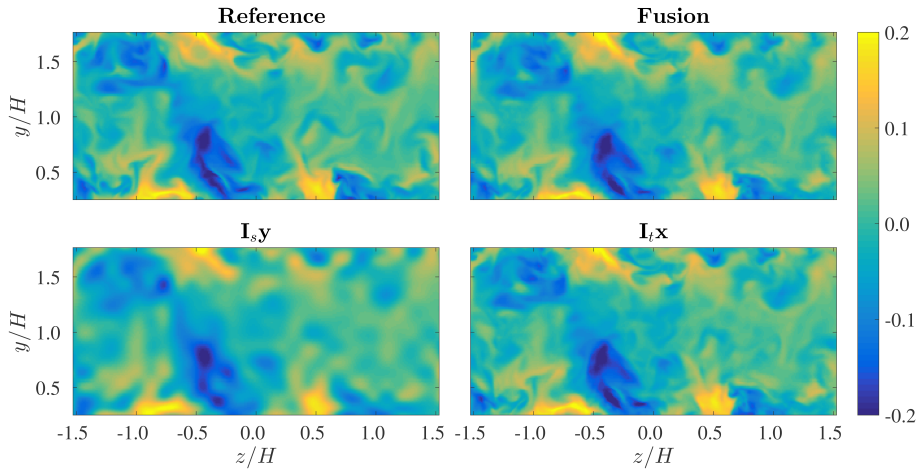
A sample velocity field, $\tau/\delta t = 2$



A sample velocity field, $\tau/\delta t = 2$

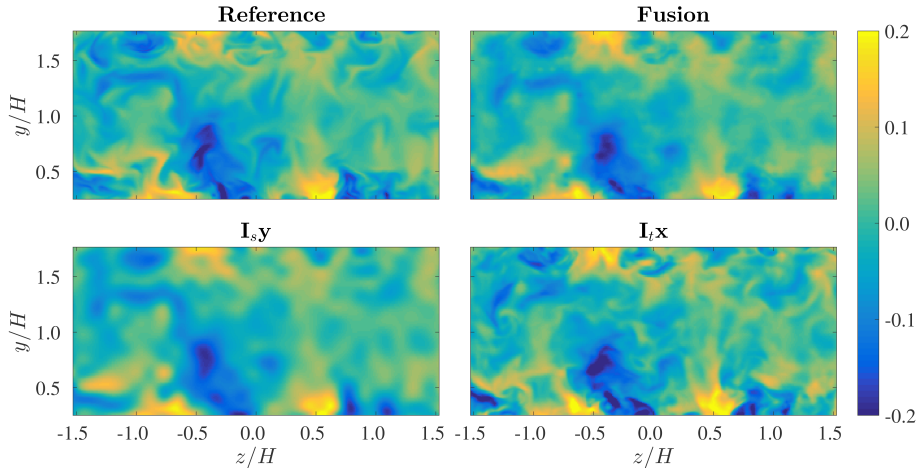


A sample velocity field, $\tau/\delta t = 2$



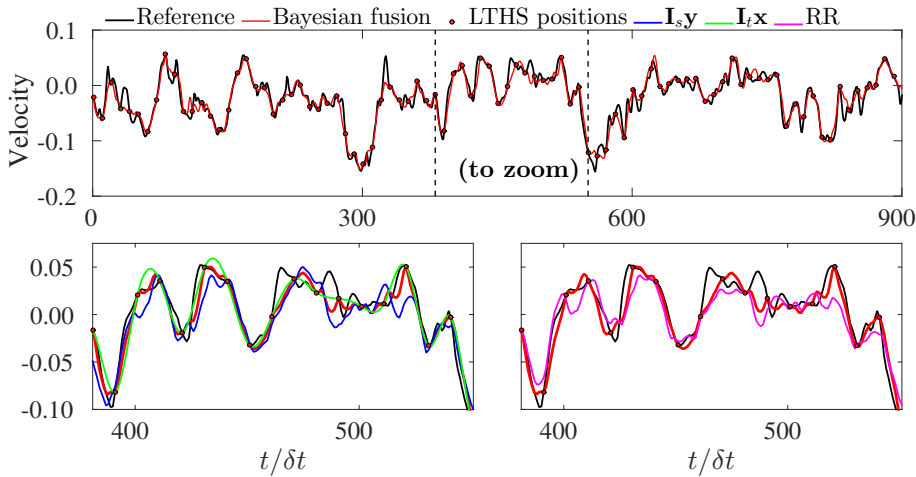
Case 2, $(P/Q, N/M) = (10^2, 10)$: reconstructed and reference streamwise velocity field at $\tau/\delta t = 2$

A sample velocity field, $\tau/\delta t = 6$



Case 2, $(P/Q, N/M) = (10^2, 10)$: reconstructed and reference streamwise velocity field at $\tau/\delta t = 6$

A sample time evolution



Case 2, $(P/Q, N/M) = (10^2, 10)$: a time evolution of reconstructed and reference streamwise velocity at the center of the channel, $y/H = 1$ and $(\alpha, \beta) = (\Delta\alpha/2, \Delta\beta/2)$

Conclusions

- ▶ Adaptive single models over-perform single interpolation methods
- ▶ Benefits are observed by combining complementary information
- ▶ Problems of sampling and aliasing should be considered in future sensing systems
- ▶ Problems in turbulence are essentially different from image processing
- ▶ Turbulence is hard, but complex learning algorithms are promising
- ▶ Learning is powerful, but physics is also crucial

Suggestions for future works

(i) On the models

- ▶ Using physical prior: Navier-Stokes, divergence-free, turbulence spectra
- ▶ Highly nonlinear mapping functions with deep neural network, potentially combined with sparse prior
- ▶ Ensemble of models: further exploit the advantages of all models
- ▶ Combine fusion and dictionary learning: ADMM

$$\mathbf{z} = \mathbf{D}\mathbf{A}s.t.\{\mathbf{D}, \mathbf{A}\} = \operatorname{argmin}_{\mathbf{D}, \mathbf{A}} \left\{ \frac{1}{2} \|\mathbf{S}_t \mathbf{D}\mathbf{A} - \mathbf{x}\|_{\Sigma_{h_t}}^2 + \frac{1}{2} \|\mathbf{S}_s \mathbf{D}\mathbf{A} - \mathbf{y}\|_{\Sigma_{h_s}}^2 + \lambda \|\mathbf{A}\|_1 \right\}$$

Suggestions for future works

(ii) Co-conception design

- ▶ Reconstruction of three-component velocity fields and cross-component quantities (cross-correlation, vorticity)
- ▶ Handle aliasing
- ▶ Increase the resolution of PIV measurements by different setups
- ▶ Design new challenging measurements

Main contributions

This work has resulted in:

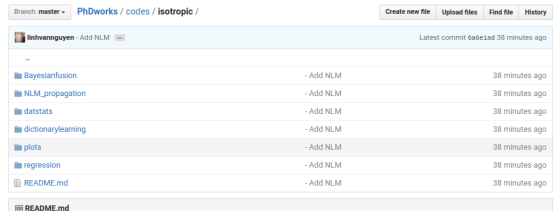
Nguyen et al., (2015). “A Bayesian fusion model for space-time reconstruction of finely resolved velocities in turbulent flows from low resolution measurements”. In: *Journal of Statistical Mechanics: Theory and Experiment* 2015.10, P10008.

and has presented at:

- ▶ 15th European Turbulence conference, Delft, Netherlands
- ▶ GDR Turbulence, Grenoble, France

Codes are available at:

<https://github.com/linhvannguyen/>



The screenshot shows a GitHub repository interface for a project named "PhDworks / codes / isotropic /". The repository was last updated 38 minutes ago. It contains several files: Bayesianfusion, NLM_propagation, datstats, dictionarylearning, plots, regression, and README.md. All files were added by the user "linhvannguyen" 38 minutes ago. Below the repository view, there is a section titled "PhD works - isotropic turbulence dataset" which provides a brief description of the project's purpose and its main parts.

PhD works - isotropic turbulence dataset

This repos synthesizes all codes and data to reproduce our results in the thesis:
Reconstruction of finely resolved velocity fields in turbulent flows from low resolution measurements

Main parts

The repos is comprised by the following main part

- Regression: linear and nonlinear regression; require `scikit-learn`
- Dictionary Learning: statistics of different learning approaches, couple dictionary learning by three post-processing techniques; require [SPAMS](<http://spams-devel.gforge.inria.fr/>)
- NLM: Matlab and C code with openMP to speedup the computation
- Bayesian fusion: code to run all cases, with step to estimate the weights
- comparison_plot: to compare all methods via NRMSE and plots
- datstats: statistics of the data

License

This project is licensed under the MIT License - see the [LICENSE.md](#) file for details

References I

-  Bonnet, J. P., Cole, D. R., Delville, J., Glauser, M. N., and Ukeiley, L. S. (1994). Stochastic estimation and proper orthogonal decomposition: complementary techniques for identifying structure. *Experiments in fluids*, 17(5):307–314.
-  Buades, A., Coll, B., and Morel, J.-M. (2005). A review of image denoising algorithms, with a new one. *Multiscale Modeling & Simulation*, 4(2):490–530.
-  Corpetti, T., Mémin, É., and Pérez, P. (2002). Dense estimation of fluid flows. *IEEE Transactions on pattern analysis and machine intelligence*, 24(3):365–380.
-  Coudert, S., Foucaut, J. M., Kostas, J., Stanislas, M., Braud, P., Fourment, C., Delville, J., Tutkun, M., Mehdi, F., Johansson, P., and George, W. K. (2011). Double large field stereoscopic piv in a high reynolds number turbulent boundary layer. *Experiments in Fluids*, 50(1):1–12.

References II

-  Dekou, R., Foucaut, J.-M., Roux, S., Stanislas, M., and Delville, J. (2016).
Large scale organization of a near wall turbulent boundary layer.
International Journal of Heat and Fluid Flow.
-  Durgesh, V. and Naughton, J. W. (2010).
Multi-time-delay lse-pod complementary approach applied to unsteady high-reynolds-number near wake flow.
Experiments in fluids, 49(3):571–583.
-  Hardie, R. C., Eismann, M. T., and Wilson, G. L. (2004).
Map estimation for hyperspectral image resolution enhancement using an auxiliary sensor.
IEEE Transactions on Image Processing, 13(9):1174–1184.
-  Papadakis, N., Mémin, É., Cuzol, A., and Gengembre, N. (2010).
Data assimilation with the weighted ensemble kalman filter.
Tellus A, 62(5):673–697.

References III

-  Protter, M., Elad, M., Takeda, H., and Milanfar, P. (2009).
Generalizing the nonlocal-means to super-resolution reconstruction.
Image Processing, IEEE Transactions on, 18(1):36–51.
-  Schneiders, J. F., Dwight, R. P., and Scarano, F. (2014).
Time-supersampling of 3d-piv measurements with vortex-in-cell simulation.
Experiments in Fluids, 55(3):1–15.
-  Tu, J. H., Griffin, J., Hart, A., Rowley, C. W., Cattafesta, L. N., and Ukeiley, L. S. (2013).
Integration of non-time-resolved piv and time-resolved velocity point sensors for dynamic estimation of velocity fields.
Experiments in fluids, 54(2):1–20.
-  Yang, J., Wright, J., Huang, T. S., and Ma, Y. (2010).
Image super-resolution via sparse representation.
IEEE transactions on image processing, 19(11):2861–2873.

Regression

Parameter estimation (regularization parameters, size of training data): *bias-variance trade-off, k-fold cross validation*

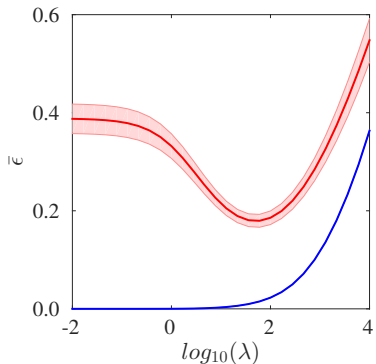


Figure: Validation curve

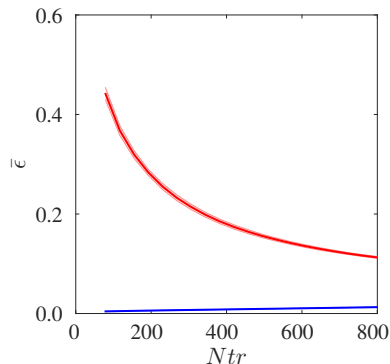


Figure: Learning curve

Dictionary learning: error vs sparsity

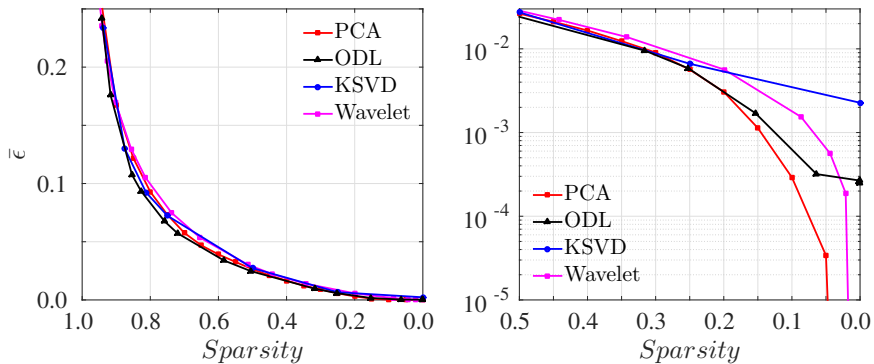


Figure: Sparsity vs error outside the training data

MAP

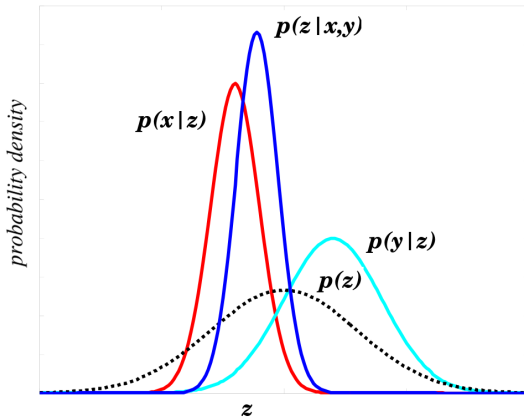


Figure: Sparsity vs error outside the training data

Pdfs of velocity increments

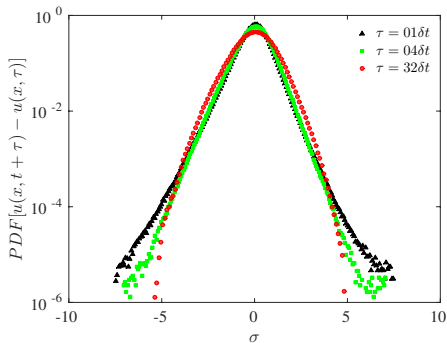
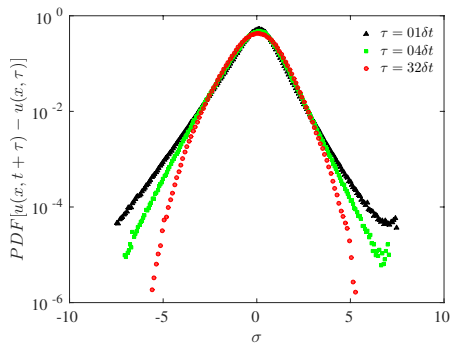


Figure: Probability density functions of velocity increments: reference and fusion

Error map

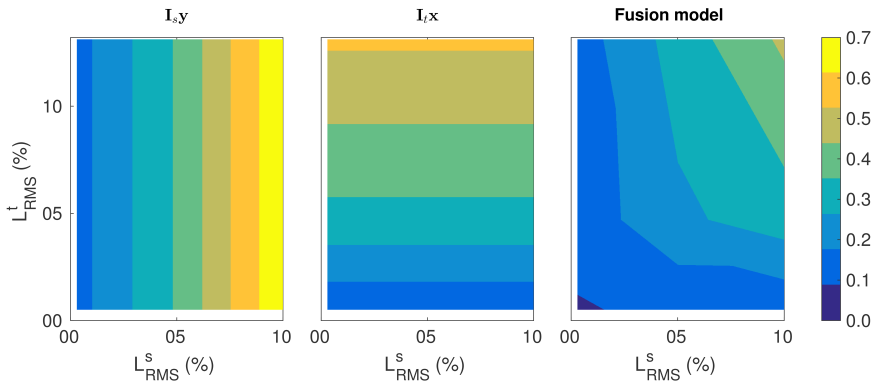


Figure: A map of errors as functions of energy losses

NLM propagation

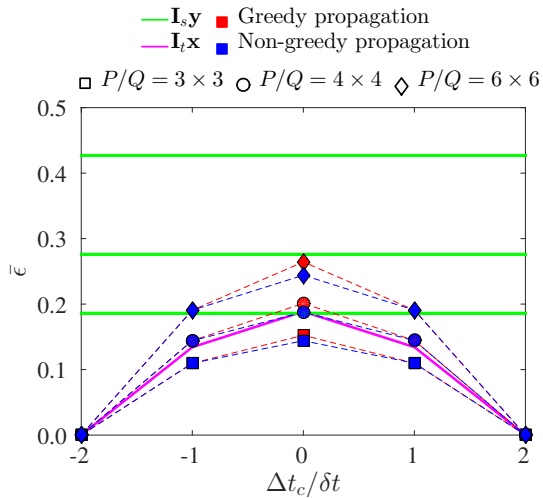


Figure: NRMSE when varying the sampling ratio in space

NLM propagation

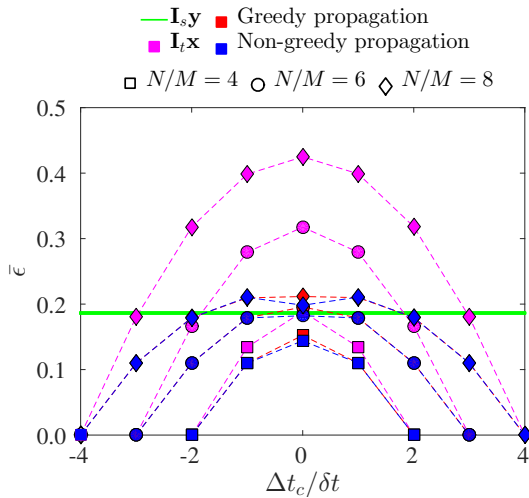


Figure: NRMSE when varying the sampling ratio in time